

Development of Bulk Ultrafine-Grained Cold Reducible Grade Low Carbon Steel Produced by Equal Channel Angular Pressing

Rajpal Singh¹, Santosh Kumar², N. K. Mukhopadhyay¹, G. V. S. Sastry¹, R. Manna^{1,*}

¹Centre of Advanced Study, Department of Metallurgical Engineering, Indian Institute of Technology (Banaras Hindu University), Varanasi Varanasi, 221 005, India

²Research and Development Centre for Iron and Steel, Steel Authority of India Limited Ispat Bhawan, Doranda, Ranchi, 834 002, India

Abstract Billets of cold reducible grade low carbon steel has been deformed at room temperature, up to an equivalent strain of 16.94, by equal-channel angular pressing (ECAP) to produce ultrafine grain (UFG) structure, adopting route Bc. Deformed microstructures are characterized by optical microscopy, transmission electron microscopy. Mechanical properties are evaluated by Vickers microhardness measurement and tensile testing. Mechanisms of grain refinement and strengthening are explored. Bulk ultrafine-grained microstructure could be produced by equal-channel angular pressing in low carbon steel. Grain refinement is strongly dependent on amount of strain. The refinement process involves several steps viz., elongation of grains by shear deformation, subdivision of grains to bands, subgrain formation in bands and fragmentation of bands into grains. Finally conversion of subgrains to grains takes place. Grain size is reduced from 68 μm to 0.20 μm twenty eight passes or an equivalent strain of 16.8. The yield and tensile strengths increase rapidly at first few passes and then reach to a saturation level. The rate of strengthening as a function equivalent strain decreases to a minimum as deformation progressed. The yield strength increases marginally by 20% but tensile strength goes up by about 300%. The major cause of strengthening is attributed to grain refinement and work hardening. However, ductility of UFG low carbon steel is lower than that of their coarse grained counterpart.

Keywords Low Carbon Steel, Equal-Channel Angular Pressing, Ultrafine Grains, Transmission Electron Microscopy, Microhardness

1. Introduction

Grain refinement is the major hardening technique that can be adopted to enhance strength in low carbon steel. Limited strengthening of steels of low carbon content can be achieved by thermomechanical treatment (TMT) due to limited refining upto 4-5 micron level[1, 2]. Ultra high strength can be achieved by grain refining to ultrafine (grain size <1 μm) level, through severe plastic deformation (SPD) method, which is an order of magnitude higher than that of TMT processes[2,3]. Heavy equipment (high tonnage) are required to process to final component size through TMT[2]. On the other hand, new processing technique called severe plastic deformation technique can deform metals and alloys repeatedly by simple shear without any change in cross-section[3-6]. Among these SPD techniques, equal-channel angular pressing can produce bulk

ultrafine-grained alloys free from any contamination, fully dense and ultrafine in grain size[3]. Steel being a major structural materials, recent research focuses on fabrication of bulk ultrafine-grained steel[1,7-22]. The grain size of low carbon steels processed by ECAP can be reduced to 0.2-0.5 μm at equivalent strain of 4 while ECAPed at 200-500°C i.e. 25 to 30 times lower than that can be achieved by TMT[1,7-9,20-21,23-24]. Grain size after ECAP at room temperature to an equivalent strain of 3 was obtained 0.2 μm [8]. The major works are either at low equivalent strain or at high temperature. Therefore, the present work focuses on producing bulk ultrafine-grained structure at high amount of equivalent strain and at room temperature.

2. Materials and Experimental Procedure

Billets of 15 mm diameter and 60-120 mm long were prepared from cold reducible grade low carbon steel plates of size 330X220X38 mm³. The plates were received from Research and Development Centre for Iron and Steel, Steel Authority of India Ltd., Ranchi, India. The steel sample was

* Corresponding author:

rmanna.met@itbhu.ac.in (R. Manna)

Published online at <http://journal.sapub.org/ijmee>

Copyright © 2013 Scientific & Academic Publishing. All Rights Reserved

analysed by optical emission spectrophotometer (OES, ARL Model 3460). The chemical composition was (by wt%) C-0.075%, Mn-0.31%, Si-0.108%, S-0.014%, P-0.033%, Al-0.028%, Ti-trace, Nb-trace and Fe-balance. The billets of 60 mm length were deformed at room temperature by ECAP adopting route Bc[3] using a 30 ton hydraulic universal testing machine. The billets were coated with a lubricant mixture of high density paraffin and MoS₂ to reduce friction between billet and die. The ECAP die consisted of two equal-channels of 15 mm diameter intersected at an inner intersection angle (Φ) 120° and an outer arc angle (Ψ) 60° that introduced an equivalent strain of ~0.6 in every passage of billet through the die. The equivalent strain ε was calculated for N number of passes by following equation[25].

$$\varepsilon = \frac{N}{\sqrt{3}} \left[2 \cot \left(\frac{\Phi}{2} + \frac{\Psi}{2} \right) + \Psi \cos ec \left(\frac{\Phi}{2} + \frac{\Psi}{2} \right) \right]$$

The billets were deformed to a maximum equivalent strain of 16.94 or 28 passes at room temperature. Deformed samples were sectioned along X, Y and Z plane for microstructural investigation. X plane was the transverse plane perpendicular to extrusion direction. Y plane was the flow plane vertical to the extruded billet and Z plane was the horizontal but parallel to top surface along extrusion direction[3]. The polished samples were etched at 2% nital solution at room temperature and the microstructure were examined using Metalux-3 optical microscope. Thin foils of 3 mm diameter and 40 μ m thickness were electropolished using an electrolyte of 10vol % perchloric acid and 90vol % methanol at 20V and at temperature at -40°C. Detailed microstructures are characterized by Tecnai20G² transmission electron microscope(TEM) at 200kV. Grain size is measured in micrographs by Heyn's linear intercept method. Hardness is measured by Shimadzu Microhardness 2T tester at varying load to find out minimum load for load independent hardness in X and Y plane for different type of samples. Based on the above result minimum load was selected as 980 mN for Vickers indenter. Tensile test was conducted on bar specimens of gauge length 16 mm and gauge diameter 4.5 mm at room temperature at a constant

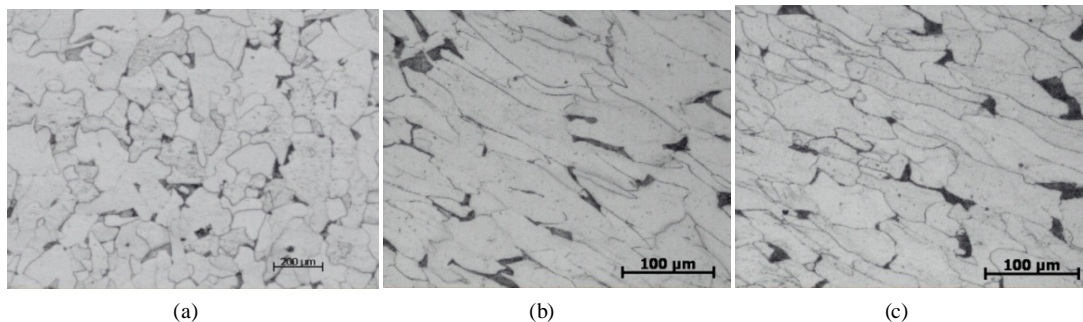
cross head speed of 0.05 cm/min and constant chart speed 2cm/min.

3. Results and Discussion

Fig. 1 shows the appearance of ECAPed samples after various degree of deformation. The sample ends are wedge shape and the angle of wedge is the shearing angle of 60°. There are no cracks while samples were deformed upto twenty seven passes (Fig 1 (a)). However a minor crack could be observed on sample that had undergone twenty eight passes of ECAP (Fig 1(b)). The extra projections at die joining face are removed before subsequent pass. The loss in length is due to this problem in die.



Figure 1. Low carbon steel billet (a) as-received, after ECAP for ten passes (P-10), fifteen passes (P-15), twenty passes (P-20) and (b) twenty eight 28 passes



(a)

(b)

(c)

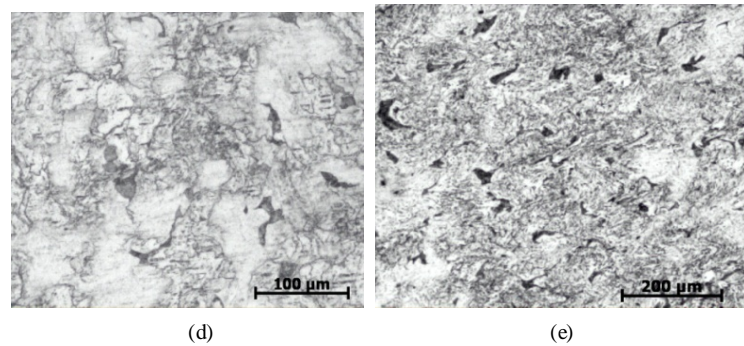


Figure 2. Optical microstructure of low carbon steel (a) as-received, after ECAP for (b) one pass, (c) two passes, (d) five passes (e) ten passes, (f) fifteen passes

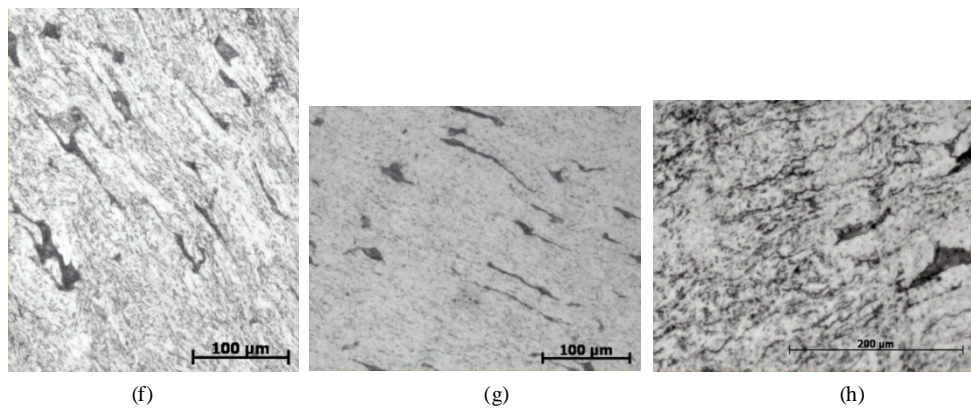


Figure 2. Optical microstructure of low carbon steel after ECAP for (f) fifteen passes, (g) twenty passes and (h) twenty eight passes

Fig 2(a) depicts the optical microstructure of as-received low carbon steel. The microstructure of as-received sample consists of mainly ferrite grains (bright contrast) with a small amount of pearlite (dark contrast). The average grain size of ferrite is found to be $68 \mu\text{m}$. Fig.2 (b)-(h) display the optical micrographs of low carbon steel of Y plane after ECAP. The grains are elongated in Y plane at initial stage of deformation (Fig 2 (b)-(c)). Average grain size decreases with amount of deformation (Fig.2 (b)-(f)). Grains subdivided to equiaxed grain/subgrain after fifteen passes. Structural modifications also took place to pearlite. Majority of lamellae were broken gradually. Cementite became spheroidised (Fig. 2(h)). However though grain size decreases with deformation but grains remains equiaxed in X plane. Bandings are not observed in X-plane.

Fig. 3 shows the bright field images of Y planes of low carbon steel after ECAP (a) two passes, (b) five passes, (c) ten passes, (d) fifteen passes, (e) twenty passes and (f) twenty eight passes. After two passes of ECAP the grains subdivided into bands (Fig. 3(a)). The microstructure contained elongated parallel bands with band width of approximate 350 nm . The band consists of elongated grains or subgrains. The average grain/subgrain size is $490 \pm 40 \text{ nm}$. The extended parallel band boundaries are called lamellar-type boundaries (LBs). The grains contained high amount of dislocations. The transition bands are also observed after two passes of ECAP (Fig.3.(b)). After five passes of ECAP the microstructure consists of elongated

grains/subgrains with good amount of dislocations (Fig. 3(c)). The average grain/subgrain size is reduced to $379 \pm 32 \text{ nm}$. The microstructure contains elongated bands of band width of 299 nm . The pearlite colonies are broken. The lamellar cementite is converted to spherical isolated cementite particles (Fig.3(d)). After ten passes the microstructure consists of elongated bands of band width of 250 nm having average grain/subgrain size of $344 \pm 28 \text{ nm}$ (Fig. 3(e)). After fifteen passes of ECAP microstructure displays ribbon grains of width 220 nm . The average grain/subgrain size is $302 \pm 20 \text{ nm}$ (Fig. 3(f)). After twenty passes microstructure depicts lower density of dislocations inside ferrite grains and the average grain size is reduced to $247 \pm 18 \text{ nm}$ (Fig. 3(g)). After twenty eight passes the average grain is reduced to $204 \pm 17.5 \text{ nm}$.

Fig. 4 depicts bright field images of X planes of low carbon steel after ECAP (a) ten passes, (b) fifteen passes, (c) twenty passes, (d) twenty eight passes. Banded structure are not observed at X plane (Fig.4(a)-(d)). However, with increasing equivalent strain or number of passes grains have got refined continuously. At the initial stages of deformation the grain consists of subgrains. After ten passes the average grain/subgrain size is $346 \pm 27 \text{ nm}$ (Fig. 4(a)). After fifteen passes the average grain/subgrain size is reduced to $290 \pm 15 \text{ nm}$ (Fig. 4(b)). At this stage majority of the boundaries are high angle boundaries. After twenty passes the average grain became $270 \pm 12 \text{ nm}$ (Fig. 4(c)). After twenty eight passes grain size reduces to $210 \pm 10 \text{ nm}$ (Fig. 4(d)).

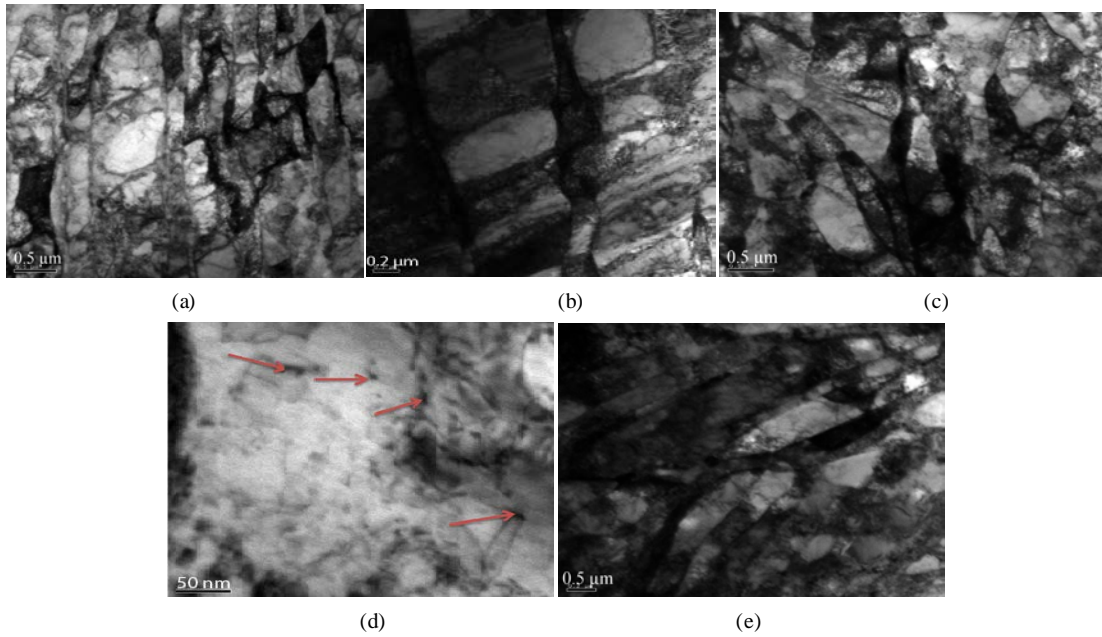


Figure 3. Bright field images of Y plane of low carbon steel after ECAP for (a)-(b) two passes, (c)-(d) five passes (arrow indicates carbide particle), (e) ten passes

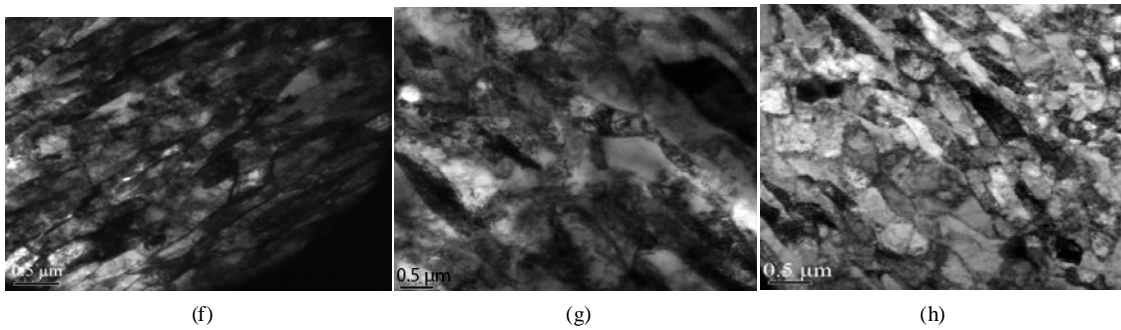


Figure 3. Bright field images of Y plane of low carbon steel after ECAP for (f) fifteen passes, (g) twenty passes and (h) twenty eight passes

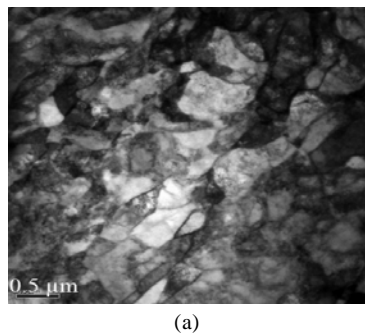


Figure 4. Bright field images of X plane of low carbon steel after ECAP for (a) ten passes

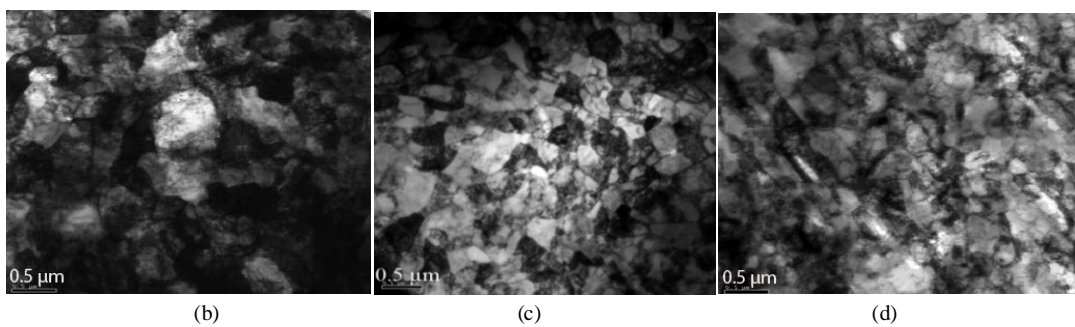


Figure 4. Bright field images of X plane of low carbon steel after ECAP for (b) fifteen passes, (c) twenty passes, (d) twenty eight passes

Fig.5 displays variation of grain/subgrain sizes at X and Y planes. The grain size decreases to 0.5 μm just after two passes of ECAP which is two orders of magnitude of starting material (average grain size 68 μm). However most of the boundaries are of low angle boundary at this stage. Results suggests that grain/subgrain size strongly depended on equivalent strain. Grain size decreases with increasing strain gradually though it has reduced at slower rate at higher strain and finally it reaches to 0.2 μm at an equivalent strain of 16.94 (twenty eight passes). The rate of decrease in grain size with increase in equivalent strain in both X and Y planes were almost identical (Fig. 5).

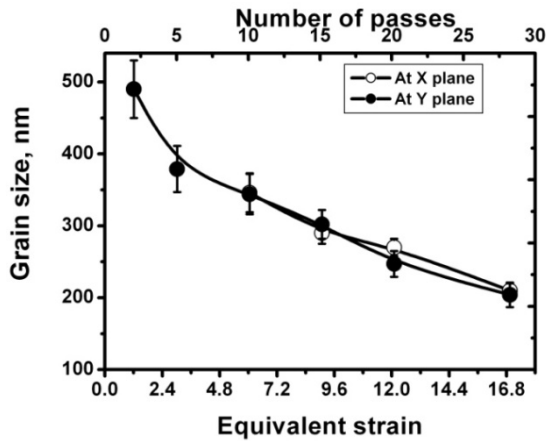


Figure 5. Variation of grain size of low carbon steel with equivalent strain

Fig. 6 shows the variation of ratio of grain/sub-grain width to its length. The ratio approaches towards unity with increasing amount of equivalent strain. However, the rate at which this ratio increases are different in X plane than that in Y plane. For a given equivalent strain this ratio is higher for X plane than that of Y plane. Therefore, grains/subgrains are more equiaxed nature in X plane than in Y plane.

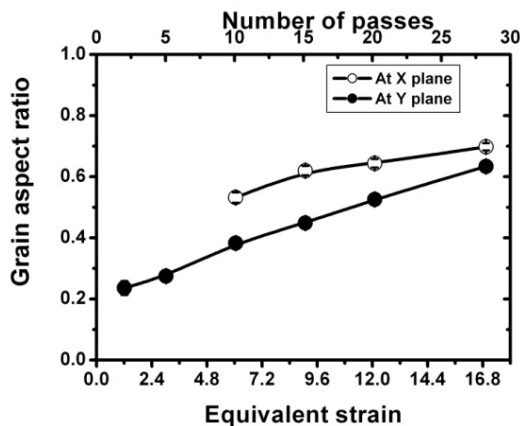


Figure 6. Variation of width to length ratio of grain/subgrain in low carbon steel with equivalent strain or number of passes

Grain refinement mechanisms operative during ECAP are explored[26,28-29] earlier for high stacking fault energy materials. At initial passes banding takes place and the thickness of the bands decreases with the number of passes. The degree of grain size reduction is highest at low

equivalent strain. Most of the boundaries at this stage are of low angle boundaries created by the rearrangement of dislocations. The grain refinement process involves (i) elongation of grains by simple shear deformation at low to intermediate equivalent strain levels, (ii) subdivision of grains to bands and subgrain formation in bands at low strain, (iii) fragmentation of bands into grains by intersection of bands due to rotation of the billet. Final microstructure contains grains with high dislocation density. This indicates that dynamic recrystallisation could not take place in low carbon steel due to continued straining by ECAP.

Fig.7 shows the engineering stress-strain curves for as-received as well as deformed samples. As-received low carbon steel yields at 225 MPa and uniformly deformed upto 27 % elongation and then necks but got fractures with a total elongation of 42%. ECAPed material yields at higher stress but quickly reaches to necking condition with a total uniform elongation of only approximately 5.5-7.5%. Ultimate tensile strength of ECAPed samples are significantly higher than that of as-received material.

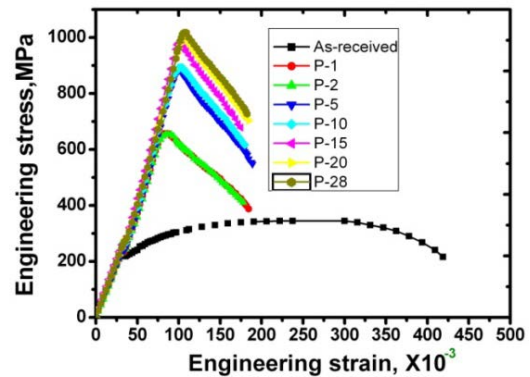


Figure 7. Engineering stress-strain curves of as-received low carbon steel and ECAPed samples

Table 1 exhibits the summary of tensile properties at room temperature for as-received as well as as-deformed samples.

Table 1. Tensile properties of as-received and ECAPed low carbon steel at room temperature [Y.S.=yield strength, U.T.S.=ultimate tensile strength, T.E.=total elongation, U.E.= uniform elongation]

Equivalent Strain	Y.S. MPa	U.T.S. MPa	T. E. (%)	U.E. (%)
0	225	344	41.88	26.9
0.6	234	656	18.48	5.47
1.21	243	653	17.81	5.63
3.02	239	882	18.90	7.03
6.05	265	892	17.97	7.19
9.08	259	983	17.50	7.19
12.10	274	1011	18.44	7.19
16.94	271	1017	18.28	7.5

Fig.8 describes variation of yield strength, ultimate tensile strength, uniform elongation and total elongation with equivalent strain.

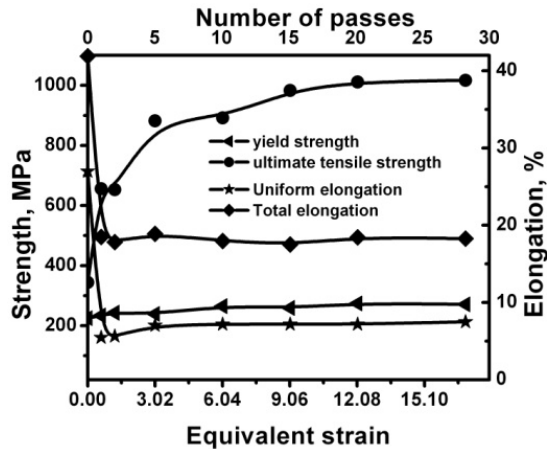


Figure 8. Variation of yield strength, ultimate tensile strength and total elongation with equivalent strain or number of passes

The yield strength of as-received low carbon steel is 225 MPa and just after one pass it increases marginally. It reaches to a saturation value of ~274 MPa. Ultimate tensile strength of ECAPed samples increases rapidly with increasing number of passes (upto 15 passes) at the initial stages of deformation or lower amount of equivalent strain and there after reaches to a saturation level at an equivalent strain of 9.1. The saturated ultimate tensile strength is about three times to that of as-received material. Fig.9 shows the variation of Vicker's microhardness (VHN) at 980 mN load with equivalent strain. The hardening behavior is very similar to the strengthening behavior. Hardness increases rapidly with increasing equivalent strain at initial stages of deformation and thereafter reaches to a saturation value which is about two and half times to that of as-received material. Hardness at X planes are very close to that at Y plane.

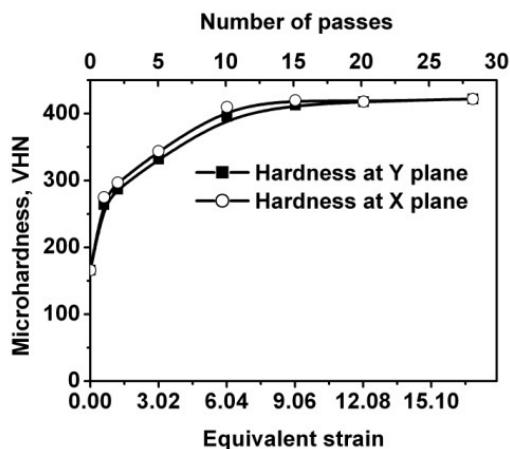


Figure 9. Variation of microhardness measured at 980 mN in X and Y-plane of ECAPed samples with equivalent strain or number of passes

The initial strengthening is due to work hardening (i.e. increase in dislocation density) and grain boundary strengthening. The rearrangement of these dislocations takes

place at higher strain to form subgrain boundaries. These boundaries have got converted to high angle boundaries at large strain. Reduction in dislocation density reduces strength nevertheless formation of high angle boundaries enhances strength by grain boundary strengthening. Though strength increases at first rate with increasing equivalent strain after few passes of ECAP at initial stage, it decreases at intermediate level and reaches a saturation level at high strain[27-28].

Results describes that both total elongation and uniform elongation decrease drastically after initial pass and remain almost constant at low value though uniform elongation regains slightly with increasing number of passes. The loss of ductility is due to lack in work hardening ability of the material[27-28]. The decrease in work hardening is due to the absorption of dislocations into non-equilibrium grain boundaries of UFG metals[30].

4. Conclusions

Equal-channel angular pressing can be adopted to produce ultrafine-grained structure in low carbon steel of average grain size of 0.2 μm . Grain refinement is strongly dependent on amount of strain. The refinement process involves several steps viz., elongation of grains by shear deformation, subdivision of grains to bands, subgrain formation in bands and fragmentation of bands into grains. Finally conversion of subgrains to grains takes place. Ultimate tensile strength of ultrafine-grained low carbon steel could be enhanced to about 1000 MPa which is about three times to that of coarse grained counterpart. The yield and tensile strengths increase rapidly at first few passes and then reach to a saturation level. The rate of strengthening as a function equivalent strain decreases to a minimum as deformation progressed. The yield strength increases marginally by 20% but tensile strength goes up to by about 300%. The major cause of strengthening is due to grain refinement and work hardening. However, ductility of UFG low carbon steel is lower than that of their coarse grained counterpart.

ACKNOWLEDGMENTS

Authors wish to thank the Department of Science and Technology, Government of India for financial support under the project no. SR/S3/ME/0009/2010 (G).

REFERENCES

- [1] R. Song, D. Ponge, D. Raabe, J.G. Speer, D.K. Matlock, Mater Sci Eng. A441 (2006) 1
- [2] V. M. Segal, Mater Sci Eng. A386 (2004) 269
- [3] R. Z. Valiev and T. G. Langdon, Prog. Mater. Sci. 51 (2006) 881

- [4] R. Z. Valiev, R. K. Islamgaliev, I. V. Alexandrov, *Prog. Mater. Sci.* 45 (2000) 103
- [5] M. Furukawa, Z. Horita, M. Nemoto, T. G. Langdon, *J. Mater. Sci.* 36 (2001) 2835
- [6] R. Manna, Ph. D. Thesis “Design and Characterization of Ultrafine-grained Aluminum and Aluminum Alloys Processed by Equal-channel Angular Pressing”, 2008, Banaras Hindu University, Varanasi, India.
- [7] D. H. Shin, B. C. Kim, Y.-S. Kim, K.-T. Park, *Acta Mater.* 48 (2000) 2247
- [8] Y. Fukuda, K. Oh-Ishi, Z. Horita, T.G. Langdon, *Acta Mater.* 50 (2002) 1359.
- [9] D. H. Shin, K. T. Park, *Mater Sci Eng. A* 410-411 (2005) 299
- [10] S. Tamimi, M. Ketabchi, N. Parvin, *Materials and Design* 30 (2009) 2556
- [11] Y. Okitsu, N. Takata, N. Tsuji *J. Mater Sc* 43 (2008) 7391
- [12] W. Lei, T. S. Wang, Z. Li, X. J. Zhang, Q. F. Wang, F. C. Zhang, *Mat. Sc. Eng A*, (2010)
- [13] M. A. Munoz-Moris, D. G. Morris, *Scripta Mater.* 63 (2010) 304
- [14] K. -T. Park, Y. S. Kim, J. G. Lee, D. H. Shin, *Mater. Sci. Eng. A* 293 (2000) 165
- [15] R. Saha, R. K. Ray, *Mater. Sci. Eng. A* 459 (2007) 223
- [16] R. Saha and R. K. Ray, *Metal Metall. Trans*, 40A (2009) 2160
- [17] A. Sarkar, A. Bhowmik and S. Suwas, *Applied Phys A*, 94(2009)943
- [18] A. Bhowmik, S. Biswas, S. Suwas, R. K. Ray, D. Bhattacharjee, *Metal Metall. Trans*, 40A (2009) 2729
- [19] T. S. Wang, Z. Li, B. Zhang, X. J. Zhang, J. M. Deng, F. C. Zhang, *Mat. Sc. Eng A*, 527 (2010) 2798
- [20] E. G. Astafurova, G. G. Zakharova, E. V. Naydenkin, S. V. Dobatkin and G. I. Raab, *The physics of Metals and Metallography*, 11 (2010) 260
- [21] Y. G. Ko, C. W. Lee, S. Namgung, D. H. Shin, *Jl. Alloys and Compounds*, 504S (2010) 5452
- [22] M. Calcagnotto, D. Ponge, D. Raabe, *Mat. Sc. Eng A*, 527 (2010) 7832
- [23] Y. II. Son, Y. K. Lee, K. T. Park, C. S. Lee, D. H. Shin, *Acta Mater* 53 (2005) 3125
- [24] K. -T. Park, S. Y. Han, B. D. Shin, Y. K. Lee, K. K. Um, *Scripta Mater* 51 (2004) 909
- [25] Y. Iwahashi, J. Wang, Z. Horita, M. Nemoto, T.G. Langdon, *Scripta Mater* 35 (1996) 143.
- [26] R. Manna, N. K. Mukhopadhyay, G. V. S. Sastry, *16th International Conference on Textures of Materials (ICOTOM 16)* December 12-17, 2011, Mumbai, India, *Mater Sci Forum* 702-703 (2012) 135.
- [27] R. Manna, N. K. Mukhopadhyay, G. V. S. Sastry, *International Conference on Advances in Metallic Materials and Manufacturing Processes for Strategic Sectors (ICAMPS 2012)*, January 19-21, 2012, Trivandrum, India, *Mater Sci Forum* 710 (2012) 241.
- [28] R. Manna, N. K. Mukhopadhyay and G. V. S. Sastry, *Metall. Mater. Trans. A*, 39A (2008) 1525
- [29] R. Manna, N. K. Mukhopadhyay and G. V. S. Sastry, *Proc. 30th Risø Intl Symp on Mat. Sci: Nanostructured Metals – Fundamentals to Applications*, edited by J.-C. Grivel et al., Risø National Laboratory for Sustainable Energy, T. U. D., Roskilde, Denmark, 7-11 Sept, 2009, P-245-252.
- [30] R. Z. Valiev, I. V. Alexandrov, T. C. Lowe, Y. T. Zhu, *J. Mater. Res.*, 17 (2002) 5